Study on Analytical Method of Energy Resolved Soft X-ray Imaging with Beryllium Filters in LHD Plasmas

Chihiro SUZUKI[1], Katsumi IDA[1], Takashi KOBUCHI[2],
Mikirou YOSHINUMA[1] and LHD Experimental Group[1]

[1]*National Institute for Fusion Science, 322-6 Oroshi-cho, Toki 509-5292, Japan*
[2]*Tohoku University, 6-6 Aoba, Aramaki, Aoba-ku, Sendai 980-8579, Japan*

In the energy resolved soft X-ray imaging carried out in LHD, two dimensional images for different photon energy ranges have been obtained by taking differences between two images measured with adjacent filter thicknesses. For the initial analysis, the dependence of the measured signal intensity on the energy range was compared with the calculated one for continuum radiation. The effects of possible errors in this analytical method have been examined in this study. The effects of the small fraction of impurities in the filter material on the signal intensity are estimated to be ignorable, while the errors of the calculated intensity due to the tolerance of the filter thickness (±10%) are expected to be larger than the other errors. Actual dispersion of the filter thickness should be precisely measured in the future. In addition, the effects of K_α lines from titanium, chromium and iron in higher energy range should be evaluated by another CCD system prepared for photon counting mode.

Keywords: soft X-ray imaging, CCD camera, beryllium filter, thickness tolerance, filter transmittance, detection efficiency, LHD

1. Introduction

Soft X-ray imaging technique using a CCD (Charge Coupled Device) camera has ever been applied to the diagnostics of magnetically confined high temperature plasmas [1, 2]. The energy resolved soft X-ray imaging has recently been carried out by changing the thickness of beryllium (Be) filter during a long pulse discharge of the Large Helical Device (LHD) [3]. This diagnostic method can possibly be applied in the future for the detection of the difference in two dimensional (2D) soft X-ray profile caused by local non-Maxwellian component of electron energy distribution function.

For the initial analysis of this experimental result, the following procedure has been applied. Firstly, 2D images for specific photon energy ranges have been obtained by taking the intensity differences between two images measured with filter pairs of adjacent thicknesses. On the other hand, the expected dependence of the signal intensity on the photon energy range has been calculated from the theoretical power spectra of continuum radiation for various electron temperatures. Finally, the dependence of the measured signal intensity on the photon energy range has been compared with the calculated ones in order to check the validity of the results, which results in rough estimation of effective (line-integrated) electron temperature.

There are several possible causes of errors in the analytical method mentioned above. According to the specification of the Be filters used in this study, small fractions of impurities are included in the filter material, and actual filter thickness may not exactly agree with the specified value (within some tolerance). The magnitude and shape of the filter transmission curve (i.e. detection efficiency curve) may be changed by these effects, which results in errors in the calculation. In addition, the slow change in the impurity radiation could occur during a long pulse discharge even if the plasma density and temperature are under steady state. Finally, the effects of line radiations which are ignored in the calculation should be considered.

In this study, the results of the energy resolved soft X-ray imaging diagnostic is discussed from the viewpoints described above. The study mainly focuses on errors in the signal intensity and the effective electron temperature evaluated from the filter specification. Though reliability of the quantum efficiency curve of the CCD chip (provided by the manufacturer) should also be considered, it is not discussed here because the measurement of the quantum efficiency curve is difficult.

author's e-mail: csuzuki@lhd.nifs.ac.jp

2. Experiment

Since the detail of the experimental setup has already been described elsewhere [3], only a brief explanation is given here. A schematic diagram of the diagnostic system installed in a tangential viewport of LHD is shown in Fig. 1. The system consists of a soft X-ray CCD camera (Andor Technology, DO435-BV) together with a pinhole, a pneumatic mechanical shutter, and a remotely rotatable filter disk which mounts 8 beryllium (Be) filters (99.8% purity). The selectable filter thicknesses are 50–1650 μm, including a common 50 μm Be window.

Figure 2 illustrates an example of the contour of the

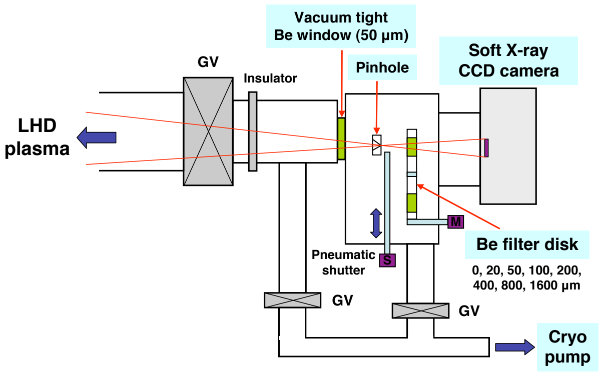

Fig. 1 Schematic diagram of the experimental setup.

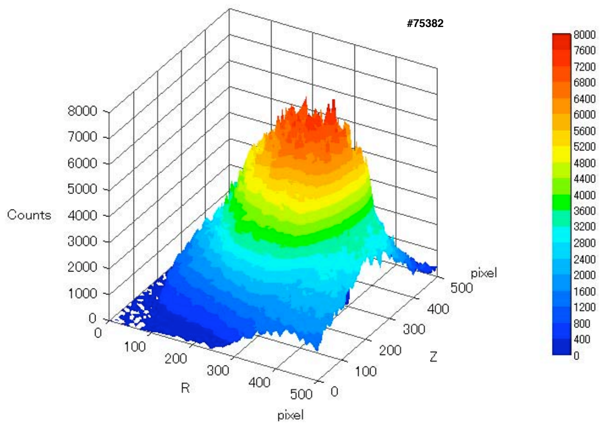

Fig. 2 Contour of the 2D image of the signal difference between the two images measured with 70 and 100 μm beryllium filters.

2D image obtained from the signal differences between the images measured with 70 and 100 μm filter thicknesses, which were obtained in a long pulse discharge sustained by ion cyclotron resonance heating (ICRH) [4]. The plasma was under quasi steady state, and the central electron temperature measured by the Thomson scattering diagnostic was about 1.3 keV at 8.9 s from the beginning of the discharge. The frame period and the exposure time of the CCD were adjusted to 10 and 5 seconds, respectively. The diameter of the pinhole was set at 0.1 mm. The hardware binning of 2×2 CCD pixels results in 512×512 superpixels in major radius (R) and vertical (Z) directions. In addition, 8×8 superpixels are averaged when the contour is drawn.

3. Detection Efficiency

The curve of overall detection efficiency versus photon energy for the signal intensity difference between the images measured with a pair of the adjacent Be filter (like Fig. 2) can be calculated from the product of the filter transmission and quantum efficiency of the CCD chip. Hence the origins of the errors in these curves may possibly affect the analytical procedure mentioned in section 1. The quantum efficiency curve of the CCD is not discussed in this article because of the reason described in section 1.

In this study, ultra-high purity beryllium foils (Grade IF-1) are used as the filters. According to the specification, the Be purity of this grade is 99.8 % (minimum), and thickness tolerance is within ±10%. The impurities of iron, beryllium oxide, aluminum, etc. are listed in the table of the small fraction of impurities in the filter material. Transmission of a filter composed of multiple materials are calculated by the formula

$$T = \exp\left(-d\rho \sum_i f_i \mu_i\right), \tag{1}$$

where d and ρ are the thickness and the mass density of the filter, and f_i and μ_i are the fraction of material mass and the mass absorption coefficient due to element i in the filter, respectively. After the detection efficiency curve of the 99.8% Be filter was calculated by including all of the impurities listed, the maximum deviation due to the thickness tolerance was estimated for the efficiency curve.

The effects of these filter specification on the overall detection efficiency curves are shown in Fig. 3, for the two combinations of the filter thicknesses (50-70 μm and 850-1650 μm). In Fig. 3(a), the curves for pure and 99.8% Be filters are plotted by broken and solid lines, respectively. As shown, the effect of the impurities becomes larger in high energy region. Slight shift of the peak of the efficiency curve is observed for higher energy range which results in the error of the peak energy of the transmittance. The effects of the purity on the magnitude of the detection efficiency are relatively small. The most influential impurities to the transmittance are iron and nickel whose fractions are 300 and 200 ppm, respectively. The structure of the absorption edges for these materials can be observed in the curve of 850-1650 μm filter combination.

On the other hand, the deviations of the transmission curves due to the tolerance of the filter thickness are drawn in Fig. 3 (b), where solid lines correspond to the exact thickness for the 99.8% Be filter and broken lines the maximum positive and negative deviations for ±10% tolerance. The effects of thickness tolerance on the magnitude of the detection efficiency are very large (≃50%) because of taking differences of the efficiency curves. The shape of the efficiency curve does not change.

4. Comparison with Calculation

Since power spectra of continuum radiations (bremsstrahlung and bound-free transitions) have dependence on photon energy (E) expressed by a factor $E\exp(-E/T_{\mathrm{e}})$, where T_{e} is an electron temperature, the dependence of signal intensity on filter combination for a given T_{e} can be calculated by integrating the product of a power spectrum and a detection efficiency curve shown in Fig. 3. As an initial step of the analyses, we

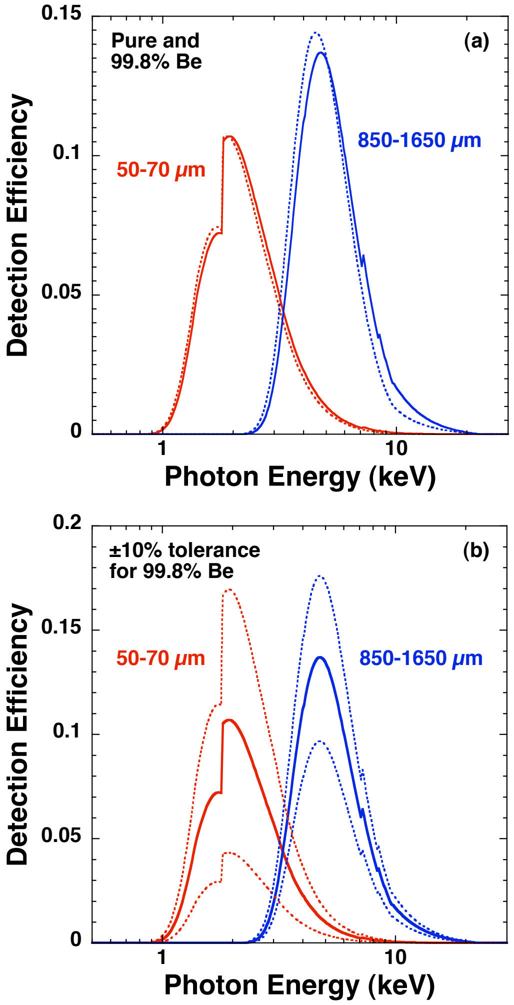

Fig. 3 Deviations of the detection efficiency curves due to (a) impurities in the filter material and (b) the thickness tolerance (±10%).

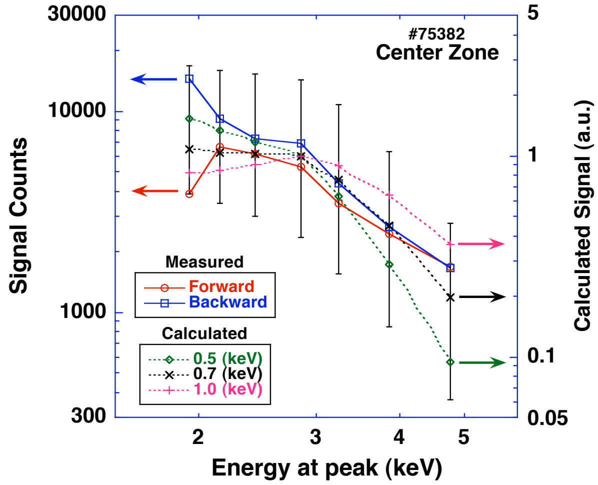

Fig. 4 The dependence of the signal intensity in the central zone (near the magnetic axis) on the photon energy range (solid lines). The horizontal axis is represented by the photon energy at the maximum efficiency for each filter combination. The calculated intensities for the electron temperatures of 0.5, 0.7 and 1.0 keV are also plotted by broken lines with the error bars due to the thickness tolerance for the case of 0.7 keV.

have compared the dependences of the measured signal intensities on filter combinations (i.e. on photon energy range) with those of the calculated ones.

The 7 images for the differences between the adjacent filters measured in the same discharge as Fig. 2 are divided into 16×16 zones by averaging in 32×32 superpixels. As for the central zone (near the magnetic axis), The measured and calculated intensities against the photon energy at the maximum efficiency for each filter combination are summarized in Fig. 4 plotted by solid and broken lines, respectively. The circle (red) and square (blue) symbols denote the experimental data in the central zone obtained by the forward and backward rotations of the filter disk, respectively, during the same shot. Therefore the disagreement between the forward and backward rotation is attributable to the slow change in the soft X-ray emission intensity from impurity ions during the discharge. The calculated intensities for the electron temperatures of 0.5, 0.7 and 1.0 keV are plotted by broken lines with the error bars due to the thickness tolerance for the case of 0.7 keV. Among the calculated intensities for the three electron temperatures, the most similar one to the experimental data is the one for 0.7 keV as plotted by times symbols (black) in Fig. 4. However, the error bars due to the thickness tolerance of the filter described above are very large. The effect of line radiations are not included in the calculation, which will be discussed in the next section.

5. Discussion

As shown in Fig. 4, inherent error in filter thickness may lead to large errors in final results due to deviation of transmission curve by taking the difference of the signals. If the vertical error bars in Fig. 4 are ignored, the effective (line-integrated) electron temperature for the central zone seems to be roughly 0.7 keV. However, the large magnitude of the error bars made it difficult to determine the temperature if the dispersion of the filter thickness would be actually ±10 %. This indicates that actual dispersion of the filter thickness, which may be smaller than 10 %, should be precisely measured (by a thickness tester) in the future for comparisons between the experimental results and the calculations. Smaller dispersions would minimize the vertical error bars.

Even if the error bars are minimized, the effects of line radiations should be discussed especially in higher energy range. Previous measurements of soft X-ray energy spectra in the Compact Helical System (CHS) by a CCD camera for photon counting mode show that K_α lines from titanium (4.8 keV), chromium (5.7 keV) and iron (6.6 keV) are significant [5]. In addition, large peaks of these three K_α lines are observed also in a similar discharge of LHD by X-ray pulse height analyzer (PHA) measurement [6]. Therefore these line radiations would influence the observed signal intensity especially in higher energy range. Another CCD camera used for the photon counting mode will also be installed in LHD in the near future as an alternative way to measure the effects of the soft X-ray line spectra.

6. Summary

We have developed a diagnostic system for the energy resolved soft X-ray imaging in a long pulse LHD discharge by using a CCD camera and Be filters with different thicknesses. Two dimensional images of soft X-ray intensity for different photon energy ranges have been obtained by taking differences between two images measured with adjacent filter thicknesses. The dependences of the measured signal intensities on the energy range were compared with the calculations for the continuum radiation. The effects of possible errors in this analytical method have been studied.

The errors due to the small fraction of impurities in the filter material are estimated to be ignorable, while the errors due to the tolerance of the filter thickness ($\pm$10%) are too large for the comparisons, which are even larger than the error due to the discharge steadiness. Actual dispersion of the filter thickness should be precisely measured for further study. In addition, the effects of K_α lines from titanium, chromium and iron in higher energy range should be studied by another soft X-ray CCD system mainly used for the photon counting mode in the near future.

Acknowledgments

This work was partly supported by a grant-in-aid for scientific research from MEXT, and the JSPS-CAS Core-University Program in the field of "Plasma and Nuclear Fusion". This work was carried out under budget code NIFS06ULBB510.

[1] Y. Liang *et al.*, Plasma Phys. Control. Fusion **44**, 1383 (2002).
[2] T. Kobuchi *et al.*, Plasma Phys. Control. Fusion **48**, 789 (2006).
[3] C. Suzuki *et al.*, *Proc. 34th EPS Conf. on Plasma Phys.*, Warsaw, 2-6 July 2007 ECA (2007) P2.139.
[4] R. Kumazawa *et al.*, Nucl. Fusion, **46**, S13 (2006).
[5] Y. Liang *et al.*, Rev. Sci. Instrum. **71**, 3711 (2000).
[6] S. Muto, S. Morita, and LHD Experimental Group, Rev. Sci. Instrum. **72**, 1206 (2001).